Spectroscopic Study of Laser-Induced Phase Transition of Gold Nanoparticles on Nanosecond Time Scales and Longer

Susumu Inasawa,*,† Masakazu Sugiyama,‡ Suguru Noda,† and Yukio Yamaguchi†

Departments of Chemical System Engineering and Electronic Engineering, School of Engineering, The University of Tokyo, Hongo 7-3-1, Bunkyo-ku, Tokyo, 113-8656, Japan

Received: December 9, 2005; In Final Form: December 26, 2005

The pulsed laser induced phase transition of gold nanoparticles in aqueous solution was observed via a transient absorption on nanosecond time scales and longer. Gold nanoparticles were excited with an intense picosecond laser pulse (355 nm, 30 ps), and the subsequent changes were monitored using two continuous wave laser wavelengths (488 and 635 nm). On the nanosecond time scale, below 6.3 mJ cm^{-2}, no change was observed; however, in the low fluence region between 6.3 and 17 mJ cm^{-2}, gold nanoparticles produced a bleach signal (488 nm) attributed to the melting of the gold nanoparticles, which decreased linearly with increasing laser fluence. Laser fluences above 17 mJ cm^{-2} resulted in a strong absorption at both wavelengths, which is ascribed to vaporization of gold nanoparticles rather than solvated electrons (ejected from gold nanoparticles) or light scattering. The decay of both signals was faster than the 5 ns time resolution used in our experimental system. On the microsecond time scale, increase in absorbance at 635 nm was observed with a time constant of 1.0 μs, while no change was observed at 488 nm. It is considered that this increase is attributed to the formation of smaller gold nanoparticles resulting from pulsed laser induced size reduction of initial gold nanoparticles.

1. Introduction

Laser light can be used to control the size and shape of nanoparticles simply by altering the fluence of the irradiating laser pulses. Since the pulsed laser induced size reduction of gold and silver nanoparticles was first discovered,[1−3] much attention has been paid to this research field, where phenomena such as the laser-induced size-controlled formation of gold nanoparticles in surfactants[4−9] and the shape transformation and size reduction of gold nanorods[10−14] have been realized. A detailed analysis of the laser-induced shape transformation[12,14,15] and size reduction[10,11,13,16−19] of gold nanoparticles has also been carried out. In our previous work, we revealed that the laser-induced shape transformation of gold nanoparticles occurs typically 100 °C below their melting point.[15] Furthermore, we also showed that the initial monomodal size distribution of gold nanoparticles becomes bimodal under picosecond pulsed laser irradiation due to the gradual size reduction of the nanoparticles.[17] Here, the size reduction of gold nanoparticles using nanosecond and picosecond laser pulses is caused by a photothermal process.[3,16,17]

These studies are mainly carried out on the basis of observed spectral changes and TEM images taken before and after laser irradiation. Although these static observations enable us to understand the irreversible changes involved in the laser-induced phenomena, the absence of dynamic information precludes a full understanding of the whole phenomenon. Owing to the advancement of experimental techniques, it is now possible to observe picosecond dynamics of electron−phonon relaxation[20] and phonon−phonon relaxation,[21−24] and even femtosecond dynamics of excited electrons.[25] Using these techniques, it has been possible to ascertain the dynamics of the shape transformation[12,26,27] and size reduction of gold nanoparticles.[28−30] For example, the shape transformation of melted gold nanorods occurs on a time scale of 30 ps[12] and is immediately followed by recrystallization of the melted nanoparticles within 5 ns after excitation.[27] Plech and co-workers irradiated gold nanoparticles with intense pulsed laser light in water and monitored the effects using small-angle X-ray scattering (SAXS). The authors observed the formation of bubbles around the nanoparticles 50 ps after excitation; these collapsed after a only few nanoseconds.[28] Francois and co-workers tested the transient absorption of the laser-induced size reduction of gold nanoparticles in a water/poly(vinyl alcohol) (PVA) mixed solution and revealed that light scattering due to vaporization and expansion of the gold nanoparticles lasted for several nanoseconds.[29,30] They also showed that bubbles formed around the hot gold nanoparticles due to heating of their surroundings. In contrast to the results of Plech and co-workers,[28] these bubbles remained in existence for several tens of nanoseconds.[30] It is considered that the solution composition affects the observed phenomenon since PVA has a low thermal conductivity and acts as an inhibitor toward thermal conduction.[30] In fact, toluene is reported to be more favorable for laser-induced size reduction than water.[19] From previous studies, the subsequent phenomenon after photoexcitation of gold nanoparticles appears strongly dependent on the properties of the surrounding media, and the observation of the transient dynamics in each solvent is essential for obtaining a fundamental understanding of these phenomena.

In this paper, we observed the transient phenomenon induced by the photoexcitation of gold nanoparticles in water by monitoring the transient absorption. We monitored both laser-induced shape transformation and size reduction, simply by changing the fluence of the laser pulses over a wide range. Melting and vaporization of gold nanoparticles, which associated

* Corresponding author. E-mail: inasawa@chemsys.t.u-tokyo.ac.jp.
† Department of Chemical System Engineering.
‡ Department of Electronic Engineering.

10.1021/jp057175l CCC: $33.50
Published on Web 02/02/2006

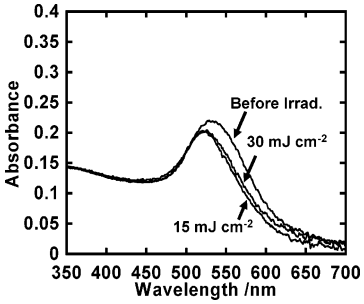

Figure 1. Absorption spectra of gold nanoparticles before and after a single pulse of laser irradiation (355 nm).

with shape transformation and size reduction, respectively, were observed. Here, nanosecond time scales and longer are used because it is hard for the widely used pump−probe method to observe transient absorption on such long time scales and few studies have been done on these time scales. The transient absorption of optically excited gold nanoparticles was observed at two different wavelengths, enabling us to gain a better understanding of what causes the change in absorbance.

2. Experimental Section

An aqueous solution of gold nanoparticles was prepared using a chemical reduction method, and the details are described elsewhere.[3,15,17,31] The atomic concentration of gold used was 0.12 mM, and the mean diameter of the nanoparticles was 36 nm. The gold nanoparticles were excited using the third harmonic of an Nd:YAG laser (EKSPLA, PL2143B) ($\lambda = 355$ nm, pulsed width = 30 ps), irradiated through a 2 mm diameter aperture. The fluence of the pump pulses was measured using a power meter (Scientech, Model 362). Two continuous wave lasers of 488 nm (National Laser Company, 800BL) and 635 nm (Sigma Koki, LDU33) wavelength were used as probes, having diameters of 1 mm or less. The probe laser light irradiated through the excited area of solutions was detected using a Si PIN photodiode (Hamamatsu, S3883), and the signals were amplified and recorded with an oscilloscope (Sony Tektronix, TDS360). A sharp-cut filter (Suruga Seiki, S79-L39) was placed in front of the photodiode to cut UV light shorter than 370 nm. To observe the dynamics induced by a single laser pulse, the solutions were flowed continuously through a quartz cell with an optical path of 5 mm.

UV−vis spectra were recorded on a multichannel detector (Hamamatsu, PMA-11) equipped with a white light source (Hamamatsu, L7893). A 50 μL volume of an aqueous solution containing 0.06 mM gold atomic concentration was placed into a quartz cell ($2 \times 10 \times 45$ mm^3, optical path 10 mm), and spectra were obtained before and after irradiating with a single laser pulse (355 nm).

Gold nanoparticles were directly observed using a transmission electron microscope (TEM) (JEOL, JEM-2010). A drop of the aqueous gold nanoparticle solution was deposited onto a carbon-coated TEM copper grid, which was then left to dry at room temperature. After drying, the carbon grids were washed with Milli-Q water to remove any remaining ionic precipitations.

3. Results

UV−vis spectra of the sample solution before and after the single pulsed laser irradiation are shown in Figure 1. Irradiation with fluences of 15 or 30 mJ cm^{-2} produced an absorption due to the surface plasmon resonance (SPR) of the gold nanoparticles centered around 520 nm. This absorption showed a clear shift to shorter wavelengths, as well as a weakened peak intensity,

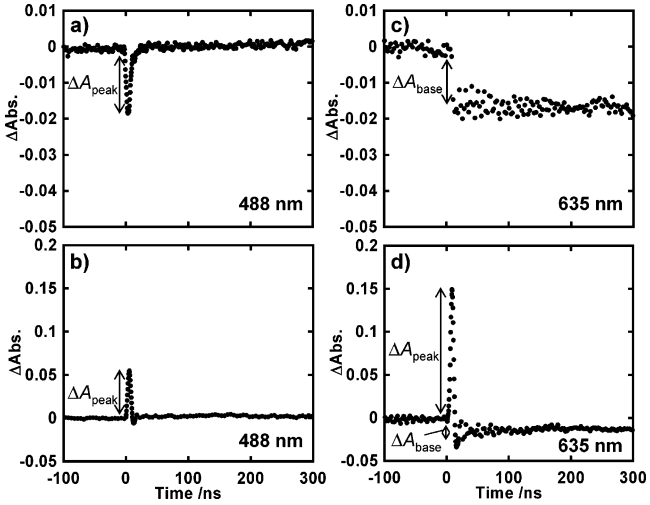

Figure 2. Typical transient absorption spectra at 488 and 635 nm on the nanosecond time scale. Irradiated laser fluences of 15 mJ cm^{-2} for (a) and (c) and 24 mJ cm^{-2} for (b) and (d) were used. ΔA_{peak} represents the value of the peak signal in the measured transient absorption, and ΔA_{base} means the difference in the absorbance at 635 nm, before and after laser irradiation.

compared to the initial spectrum. These changes in absorption are consistent with previously reported work,[3,4,14,15,17] indicating that laser-induced shape transformation or size reduction of the gold nanoparticles has occurred. Irradiation of the sample with laser energy of 30 mJ cm^{-2} produces a slightly stronger absorption in the red region than that with energy of 15 mJ cm^{-2}. The identification of this absorption is discussed later. Absorbances below 500 nm showed little change because the absorption originated in the interband transition (5d → 6sp),[32] which is insensitive to the size and shape of the nanoparticles.[9,13]

Figure 2 shows typical transient absorption spectra for irradiated gold nanoparticles obtained at 488 and 635 nm on the nanosecond time scale. Irradiation with a laser energy of 15 mJ cm^{-2} produced a sharp decrease in absorbance at 488 nm (Figure 2a), suggesting that the gold nanoparticles became transparent due to photoexcitation. The negative signal decayed faster than the 5 ns time resolution of the experimental system. At 635 nm, however, the absorbance decreased instantaneously and remained constant for 300 ns (Figure 2c). A more intense pulse of 24 mJ cm^{-2} produced positive absorbance changes at both wavelengths (Figure 2b,d), which were observed to decay quickly over a 5 ns time scale. The contrasting sign of the peak signal in the transient absorption is a good indication that different phenomena occur with high laser intensity. With the larger fluence (24 mJ cm^{-2}), the observed absorbance after the instantaneous decrease at 635 nm also remained constant (Figure 2d). As an intermediate signal between the positive and negative peaks shown in Figure 2a,b, both peaks were observed at the same time with a laser fluence of 22 mJ cm^{-2} (Figure 3). The signal appeared to be the summation of both negative and positive peaks (Figure 3), indicating that both phenomena occurred at this fluence. This intermediate signal was only observed for a fluence of 22 mJ cm^{-2}.

The values of the peak signals (ΔA_{peak}) in Figure 2 were plotted in Figure 4. At 488 nm, ΔA_{peak} was found to decrease with increasing laser fluence up to around 18 mJ cm^{-2}. Above this fluence, in turn, ΔA_{peak} increased as the fluence increased and changed in sign above 24 mJ cm^{-2} (Figure 4a). The inset in Figure 4a shows negative values of ΔA_{peak} at 488 nm in the low fluence region. They decreased almost linearly above the threshold energy of 6.3 mJ cm^{-2} (Figure 4a). At 635 nm, no

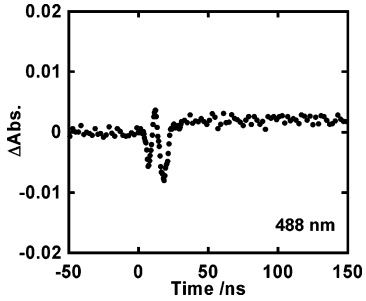

Figure 3. Intermediate signal observed at 488 nm with a laser fluence of 22 mJ cm^{-2}. Both negative and positive absorbance changes were observed.

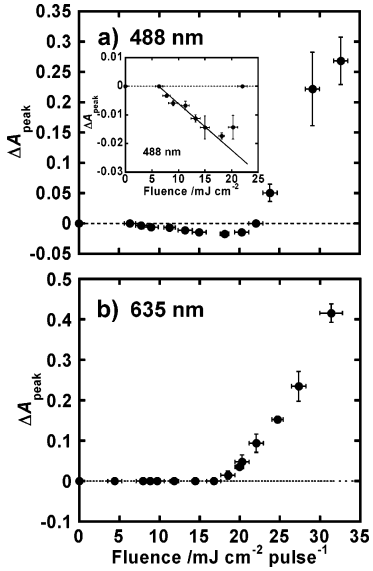

Figure 4. ΔA_{peak} versus laser fluence. The dotted line indicates the zero position. The inset shows ΔA_{peak} at 488 nm in low fluence region. The solid line in the inset was the linear fitting result to the experimental data between 6.3 and 18 mJ cm^{-2}. Note that the intermediate signal at 22 mJ cm^{-2} was plotted as zero in part a.

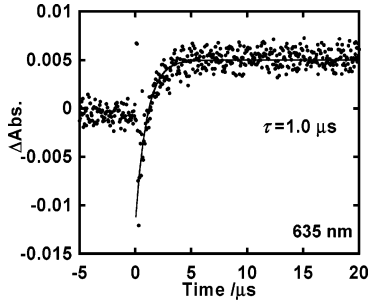

Figure 5. Time evolution of absorbance at 635 nm on the microsecond time scale using a laser fluence of 28 mJ cm^{-2}. The solid line is the fitting result by one exponential function $\propto (1 - \exp(-t/\tau))$ with a time constant $\tau = 1.0$ μs.

peak was observed up to 17 mJ cm^{-2}, while above that ΔA_{peak} increased rapidly with increase in laser fluence (Figure 4b). Note that ΔA_{peak} at 22 mJ cm^{-2} is plotted as 0 in Figure 4a because both negative and positive peaks are observed at the same time; neither can be used to define ΔA_{peak} in the same manner as the other data.

When laser fluences greater than 20 mJ cm^{-2} were used, distinct increases in the transient absorption were observed after the instantaneous decrease in absorbance at 635 nm on a microsecond time scale (Figure 5). No absorbance change was observed at 488 nm on this time scale. The time evolution of

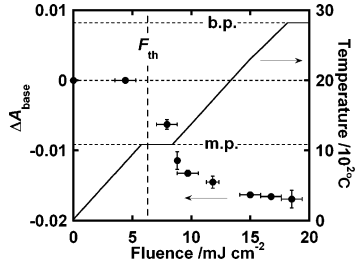

Figure 6. ΔA_{base} at 635 nm plotted in terms of laser fluence. An estimation of the particle temperature is also shown (solid line). In this figure, the lines "m.p." and "b.p." correspond to the melting point and boiling point, respectively, of bulk gold. F_{th} is the threshold energy of 6.3 mJ cm^{-2} for negative changes in absorbance at 488 nm.

the absorbance was fitted to one exponential function $\propto (1 - \exp(-t/\tau))$ (Figure 5). The time constant of the increase, τ, was determined to be 1.0 μs, and it showed little dependence on the irradiated laser fluence.

4. Discussion

4.1. Origin of Negative Absorbance Changes. The absorbance changes (ΔA_{base}) at 635 nm in Figure 2, observed around the fluence threshold of 6.3 mJ cm^{-2}, are plotted in Figure 6. As seen in Figure 1, the absorbance in the red region shows a decrease after a single pulse of laser irradiation, resulting from the shape transformation of the gold nanoparticles to form spheres or from particle size reduction.[3,12,15,17] Therefore, ΔA_{base} at 635 nm corresponds to the shape transformation or size reduction of the gold nanoparticles. Since the laser-induced shape transformation and size reduction of gold nanoparticles occurs on 30 ps[12] and subnanosecond time scales,[29,30] respectively, which is faster than the time resolution used in our system, then only an abrupt decrease in the absorbance (ΔA_{base}) at 635 nm is observed, as shown in Figure 2c,d. In Figure 6, while no change was observed below 4 mJ cm^{-2}, ΔA_{base} decreased with increases in fluence greater than 8 mJ cm^{-2}, meaning that a threshold also exists between 4 and 8 mJ cm^{-2} for ΔA_{base}. This result indicates that negative changes of ΔA_{peak} at 488 nm and ΔA_{base} at 635 nm were caused by the same phenomenon. An estimation of the particle temperature showed that a laser pulse with fluence between 6 and 8.4 mJ cm^{-2} is sufficient to heat the gold nanoparticles to their melting point (Figure 6). Here, adiabatic conditions were assumed, because the time constant of heat dissipation from the particles is 100−200 ps,[23] which is larger than the pulse duration (30 ps) of the pump laser used. From these results, we conclude that the threshold value of 6.3 mJ cm^{-2} for negative absorbance change corresponds to the melting of the gold nanoparticles. Our results also indicate that, around 488 nm, melted gold nanoparticles have a smaller absorption coefficient than that of solid gold nanoparticles. The observation of a bleach signal in the transient absorption process can help us to determine whether the excited gold nanoparticles have melted.

4.2. Origin of Positive Absorbance Changes. Above 17 mJ cm^{-2}, the positive absorbance change becomes dominant. Three possibilities can be considered as its origin: (1) solvated electrons ejected from the gold nanoparticles; (2) vaporization of gold nanoparticles; (3) scattering of light due to some scattering center. If the origin is light scattering, then taking Rayleigh scattering into account, a stronger scattering is expected at shorter wavelengths. However, as seen in Figure 4, the absorbance at 635 nm is larger than that at 488 nm in the fluence region above 24 mJ cm^{-2}, implying that light scattering is not responsible for the observed change.

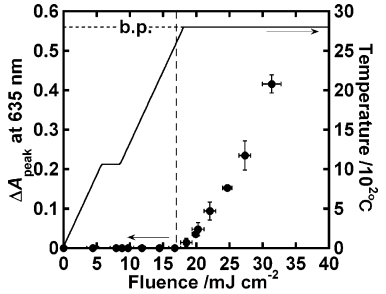

Figure 7. Estimated temperature of gold nanoparticles and ΔA_{peak} at 635 nm. In this figure, "b.p." means the boiling point of gold. The vertical dashed line corresponds to the threshold energy of 17 mJ cm^{-2}.

It is well-known that solvated electrons show strong broad absorption in the red region,[33−37] and that electrons are ejected from silver nanoparticles by intense pulse irradiation.[38] We checked this probability by a simple estimation. Since excited electrons in aqueous solution relax into the ground state within 1 ps,[36] if the observed absorption was due to solvated electrons, then the corresponding absorption spectrum of solvated electrons at the equilibrium state would be obtained. At 635 nm, the absorption coefficient of solvated electrons in water, $\epsilon_{electron}$, at equilibrium is about 1.7×10^4 M^{-1} cm^{-1},[35−37] and the number of solvated electrons, $n_{electron}$ can be calculated using the data in Figure 4b. The number of electrons, $n_{electron}$, is obtained as

$$n_{electron} = \frac{\Delta A_{peak} N_A}{l \epsilon_{electron}} \quad (1)$$

where N_A is Avogadro's constant and l is the path length (0.5 cm). $n_{electron}$ is estimated to be $1 \times 10^{15}-3 \times 10^{16}$ electrons per cubic centimeter on the basis of ΔA_{peak} at 635 nm (Figure 4b). The number of gold nanoparticles in our aqueous solution is estimated as 5×10^{10} particles per cubic centimeter. Hence, about $2 \times 10^4-6 \times 10^5$ electrons should be ejected from a single gold nanoparticle. The number of free electrons in a single gold nanoparticle is estimated as 1.4×10^6, using a bulk vaule of 5.9×10^{22} cm^{-3}.[39] That is, up to 43% of free electrons should be ejected from a single gold nanoparticle. Because the work function of gold is 5.3 eV,[40] which is larger than the excitation source (3.5 eV), two-photon absorption is required for electron ejection. However, in our system, one-photon absorption was dominant and hence electron ejection was less expected. Even if electron ejection would occur, it is considered that the work function of gold nanoparticles increases with the increase of number of ejected electrons because electrons should be removed from "cationic" gold nanoparticles. In fact, the first and second ionization energies of gold atom are 9.22 and 20.5 eV, respectively,[40] and it is considered that much larger energy than the work function of "neutral" nanoparticles is required to remove electrons from "cationic" ones. From the discussion above, electron ejection up to 43% of free electrons from gold nanoparticles is less expected using pulsed laser light of 3.5 eV. Therefore we ruled out the possibility of solvated electrons.

In Figure 7, a set of data of ΔA_{peak} at 635 nm was compared to estimated temperature of gold nanoparticles. The threshold energy of 17 mJ cm^{-2} is just below the laser fluence required for the heating of gold nanoparticles to the boiling point. At the threshold, the particle temperature is about 2500 °C and gold vapor with pressure of larger than 10^4 Pa is formed,[40] suggesting that gold vapor formation is responsible for positive absorbance change at 635 nm. We considered that positive changes in absorbance were caused by vaporization of gold nanoparticles due to laser heating.

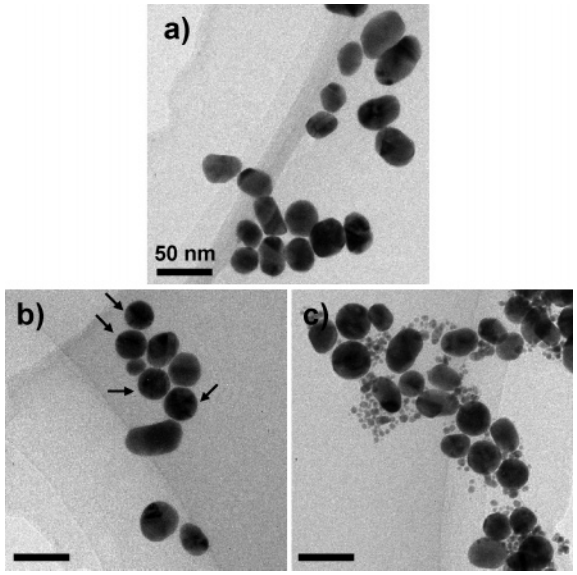

Figure 8. TEM images of gold nanoparticles before (a) and after one pulse irradiation of 15 (b) and 32 mJ cm^{-2} (c). Arrows in (b) indicate spherical gold nanoparticles.

If more intense laser light than the one used is employed in our system, electron ejection or ionization of gold atoms might be observed because the size reduction of gold nanoparticles caused by Coulomb explosion would occur under intense femtosecond laser pulses.[13] In addition, irradiation of spherical silver nanoparticles embedded in soda lime glass with intense femtosecond laser pulses causes ionization of silver atoms, resulting in the deformation of the nanoparticles to oblong shapes.[41,42] These phenomena are caused by laser pulses with ca. 1−3 orders of intensity higher than ours.[13,41,42] Therefore, it is considered that electron ejection or ionization of gold atoms would be dominant and the laser-induced phase transition observed here would be less expected under ultrafast laser pulses with high intensity.

Because negative and positive changes in absorbance were ascribed to phase transition of gold nanoparticles to liquid and vapor, corresponding shape/size changes of nanoparticles were expected. Spherical nanoparticles are formed by melting, and small nanoparticles are formed by vaporization of nanoparticles. Figure 8 shows TEM images of gold nanoparticles before and after 1 pulse irradiation. Irradiated laser fluence of 15 mJ cm^{-2} (Figure 8b) and 32 mJ cm^{-2} (Figure 8c) correspond to melting and vaporization of gold nanoparticles, respectively. Spherical and small nanoparticles were clearly confirmed in Figure 8b,c, which also supports our interpretation of transient absorption.

4.3. Formation of Small Nanoparticles on a Microsecond Time Scale. In Figure 5, an increase in absorbance was observed with a time constant of 1.0 μs. Since no change was observed at 488 nm on this time scale, we infer that scattering is not responsible for the observed increase in absorbance. The possibility of the origin being solvated electrons is also eliminated, because, in addition to the discussion in section 4.2, the time constant corresponding to electron ejection from silver nanoparticles was reported as 1.5 ns,[38] which is 3 orders smaller than the time constant obtained here. The increase in absorbance is explained by the formation of small gold nanoparticles. Gold nanoparticles smaller than 2.5 nm have large absorption coefficients in the red region,[4,6,8,9] and the formation of small gold nanoparticles is clearly confirmed by the TEM images shown in Figure 8c. As already described, we did not observe the increase in absorbance at 635 nm on the microsecond time

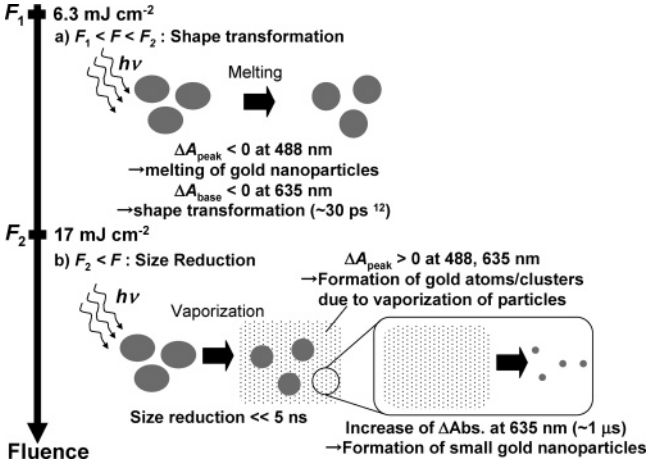

Figure 9. Schematic features of laser-induced phase transition.

scale at fluences lower than 20 mJ cm^{-2}. This observation is also explained by the lack of formation of small gold nanoparticles in the lower fluence region. Furthermore, through the observation of laser-induced size reduction of gold nanoparticles by SAXS, the formation of small gold clusters with about 2 nm diameter is reported to occur over a few microseconds.[28] Therefore, the observed increase in absorbance at 635 nm is attributed to the formation of small gold nanoparticles after laser-induced size reduction.

A slightly stronger absorption is observed in the red region for a fluence of 30 mJ cm^{-2} compared to that of 15 mJ cm^{-2} (see Figure 1), which is explained by the formation of small nanoparticles. Since small gold nanoparticles are formed at 30 mJ cm^{-2}, but scarcely formed at 15 mJ cm^{-2}, the former results in a slightly stronger absorption in the red region. While the absorbance at 635 nm is found to be larger in the transient absorption after irradiation than that of the initial one as shown in Figure 5, in the UV−vis spectra the absorbance of the sample irradiated with a fluence of 30 mJ cm^{-2} in the red region is smaller than that of the initial solution (Figure 1), which is due to the growth of small gold nanoparticles. Since it took a few minutes to measure the UV−vis spectra after irradiation, the small nanoparticles were able to increase their sizes through aggregation, causing the absorbance in the red region to decrease, as reported previously.[4,6]

Our whole understanding of the laser-induced phase transition of gold nanoparticles is summarized in Figure 9. Above 6.3 mJ cm^{-2}, melting of gold nanoparticles is observed as bleach signals of ΔA_{peak} at 488 nm. The nanoparticles in this region are able to alter their shape to form spheres on a time scale of 30 ps,[12] resulting in negative changes of ΔA_{base} at 635 nm. Above 17 mJ cm^{-2}, gold nanoparticles are heated to the point of significant vaporization, leading to positive changes of ΔA_{peak} at both wavelengths and subsequent size reduction of the gold nanoparticles. The time constants of both melting and vaporization were faster than the 5 ns time resolution used. After the observed size reduction of the gold nanoparticles, formation of small gold nanoparticles is observed as the increase of absorbance at 635 nm with a time constant of 1.0 μs.

5. Conclusion

The transient absorption of laser-excited gold nanoparticles was observed at two different wavelengths, 488 and 635 nm. Fluences below 6.3 mJ cm^{-2} resulted in no change in the transient absorption; however, for fluences between 6.3 and 17 mJ cm^{-2}, bleach signals (ΔA_{peak} at 488 nm) were observed as a result of melting of gold nanoparticles. In this fluence region, negative changes of ΔA_{base} were also observed at 635 nm due to the shape transformation of gold nanoparticles. Above 17 mJ cm^{-2}, strong absorption ($\Delta A_{peak} > 0$) at both wavelengths was observed due to vaporization of gold nanoparticles. While no change was observed at 488 nm, an increase in absorbance at 635 nm was observed on the microsecond time scale for fluences larger than 20 mJ cm^{-2}. It is considered that this increase in absorbance originates from the formation of small gold nanoparticles after laser-induced size reduction of initial gold nanoparticles.

Acknowledgment. This work was supported by Research Fellowships of the Japan Society for the Promotion of Science (JSPS) for Young Scientists and the "Nanotechnology Materials Programs-Nanotechnology Particle Project" of the New Energy and Industrial Technology Development Organization (NEDO) based on funds provided by the Ministry of Economy, Trade and Industry, Japan (METI). We thank Dr. H. Yui, Tokyo University of Science, for his technical support for the laser equipment. We also thank the High Voltage Electron Microscope Laboratory, School of Engineering, The University of Tokyo, for their technical support for TEM.

References and Notes

(1) Takami, A.; Yamada, H.; Nakano, K.; Koda, S. *Jpn. J. Appl. Phys.* **1996**, *35*, L781.
(2) Kurita, H.; Takami, A.; Koda, S. *Appl. Phys. Lett.* **1998**, *72*, 789.
(3) Takami, A.; Kurita, H.; Koda, S. *J. Phys. Chem. B* **1999**, *103*, 1226.
(4) Mafune, F. *Chem. Phys. Lett.* **2004**, *397*, 133.
(5) Mafune, F.; Kondow, T. *Chem. Phys. Lett.* **2003**, *372*, 199.
(6) Mafune, F.; Kohno, J.; Takeda, Y.; Kondow, T. *J. Phys. Chem. B* **2002**, *106*, 8555.
(7) Mafune, F.; Kohno, J.; Takeda, Y.; Kondow, T. *J. Phys. Chem. B* **2001**, *105*, 5114.
(8) Mafune, F.; Kohno, J.; Takeda, Y.; Kondow, T. *J. Phys. Chem. B* **2002**, *106*, 7575.
(9) Mafune, F.; Kohno, J.; Taketa, Y.; Kondow, T. *J. Phys. Chem. B* **2001**, *105*, 9050.
(10) Chang, S.-S.; Shih, C.-W.; Chen, C.-D.; Lai, W.-C.; Wang, C. R. C. *Langmuir* **1999**, *15*, 701.
(11) Link, S.; Burda, C.; Hohamed, M. B.; Nikoobakht, B.; El-Sayed, M. A. *J. Phys. Chem. A* **1999**, *103*, 1165.
(12) Link, S.; Burda, C.; Nikoobakht, B.; El-Sayed, M. A. *Chem. Phys. Lett.* **1999**, *315*, 12.
(13) Link, S.; Burda, C.; Nikoobakht, B.; El-Sayed, M. A. *J. Phys. Chem. B* **2000**, *104*, 6152.
(14) Link, S.; El-Sayed, M. A. *J. Chem. Phys.* **2001**, *114*, 2362.
(15) Inasawa, S.; Sugiyama, M.; Yamaguchi, Y. *J. Phys. Chem. B* **2005**, *109*, 3104.
(16) Inasawa, S.; Sugiyama, M.; Koda, S. *Jpn. J. Appl. Phys., Part 1* **2003**, *42*, 6705.
(17) Inasawa, S.; Sugiyama, M.; Yamaguchi, Y. *J. Phys. Chem. B* **2005**, *109*, 9404.
(18) Kawasaki, M.; Masuda, K. *J. Phys. Chem. B* **2005**, *109*, 9379.
(19) Peng, Z.; Walther, T.; Kleinermanns, K. *J. Phys. Chem. B* **2005**, *109*, 15735.
(20) Hodak, J. H.; Martini, I.; Hartland, G. V. *J. Phys. Chem. B* **1998**, *102*, 6958.
(21) Hu, M.; Petrova, H.; Hartland, G. V. *Chem. Phys. Lett.* **2004**, *391*, 220.
(22) Hu, M.; Hartland, G. V. *J. Phys. Chem. B* **2002**, *106*, 7029.
(23) Hodak, J. H.; Henglein, A.; Giersig, M.; Hartland, G. V. *J. Phys. Chem. B* **2000**, *104*, 11708.
(24) Shin, H. J.; Hwang, I.-W.; Hwang, Y.-N.; Kim, D.; Han, S. H.; Lee, J.-S.; Cho, G. *J. Phys. Chem. B* **2003**, *107*, 4699.
(25) Fann, W. S.; Storz, R.; Tom, H. W. K.; Bokor, J. *Phys. Rev. B* **1992**, *46*, 13592.
(26) Hartland, G. V.; Hu, M.; Sader, J. E. *J. Phys. Chem. B* **2003**, *107*, 7472.
(27) Plech, A.; Kotaidis, V.; Gresillon, S.; Damen, C.; von Plessen, G. *Phys. Rev. B* **2004**, *70*, 1954230.
(28) Plech, A.; Kotaidis, V.; Lorenc, M.; Wulff, M. *Chem. Phys. Lett.* **2005**, *401*, 565.
(29) Francois, L.; Mostafavi, M.; Belloni, J.; Delouis, J.-F.; Delaire, J.; Feneyron, P. *J. Phys. Chem. B* **2000**, *104*, 6133.

(30) Francois, L.; Mostafavi, M.; Belloni, J.; Delaire, J. A. *Phys. Chem. Chem. Phys.* **2001**, *3*, 4965.

(31) Kreibig, U.; Vollmer, M. *Optical Properties of Metal Clusters*; Springer: Berlin, 1995.

(32) Alvarez, M. M.; Khoury, J. T.; Schaaff, T. G.; Shafigullin, M. N.; Vezmar, I.; Whetten, R. L. *J. Phys. Chem. B* **1997**, *101*, 3706.

(33) Crowell, R. A.; Lian, R.; Shkrob, I. A.; Qian, J.; Oulianov, D. A.; Pommeret, S. *J. Phys. Chem. A* **2004**, *108*, 9105.

(34) Assel, M.; Laenen, R.; Laubereau, A. *Chem. Phys. Lett.* **1998**, *289*, 267.

(35) Assel, M.; Laenen, R.; Laubereau, A. *J. Chem. Phys.* **1999**, *111*, 6869.

(36) Assel, M.; Laenen, R.; Laubereau, A. *J. Phys. Chem. A* **1998**, *102*, 2256.

(37) Kloepfer J. A.; Vilchiz, V. H.; Lenchenkov, V. A.; Germaine, A. C.; Bradforth, S. E. *J. Chem. Phys.* **2000**, *113*, 6288.

(38) Kamat, P. V.; Flumiani, M.; Hartland, G. V. *J. Phys. Chem. B* **1998**, *102*, 3123.

(39) Kittel, C. *Introduction to Solid State Physics*, 7th ed.; John Wiley and Sons: New York, 1996.

(40) *Handbook of Chemistry and Physics*, 83rd ed.; CRC Press: Boca Raton, FL, 2002.

(41) Kaempfe, M.; Seifert, G.; Berg, K.-J.; Hofmeister, H.; Graener, H. *Eur. Phys. J. D* **2001**, *16*, 237.

(42) Podlipensky, A. V.; Grebenev, V.; Seifert, G.; Graener, H. *J. Lumin.* **2004**, *109*, 135.